Vision Res. Vol. 28, No. 10, pp. 1095–1105, 1988
Printed in Great Britain.

0042-6989/88 $3.00 + 0.00

GENERATION OF THE *e*-WAVE OF THE ELECTRORETINOGRAM IN THE FROG RETINA

CHESTER J. KARWOSKI and ERIC A. NEWMAN[1]

Vision Research Laboratory, Department of Psychology, University of Georgia, Athens, GA 30602,
Department of Physiology, University of California, San Francisco, CA 94143 and
[1]Eye Research Institute of Retina Foundation, 20 Staniford St., Boston, MA 02114, U.S.A.

(*Received* 27 *July* 1987; *in revised form* 29 *December* 1987)

Abstract—The *e*-wave and a delayed-OFF increase in extracellular K^+ concentration are both maximum in the distal half of the inner plexiform layer. These responses also have similar latency, time-course, intensity-dependence, surround properties, and sensitivity to tetrodotoxin. Current source-density analysis of the *e*-wave reveals a current sink through the proximal retina, a source at the retinal surface, and, in some cases, a weaker source in the mid-retina. These results suggest a model for *e*-wave generation: delayed-OFF activity in proximal neurons releases K^+, which enters Muller cells in the inner plexiform layer; a current exits Muller cells primarily via their endfeet, and the return flow through extracellular space produces the *e*-wave.

Rana pipiens Electroretinogram K^+ selective microelectrode Tetrodotoxin Current source density analysis

INTRODUCTION

Light-evoked field potentials recorded within the retina are of interest because they have provided insights regarding both retinal function and the origins of the transretinally-recorded electroretinogram (ERG). The *e*-wave is a delayed-OFF intraretinal field potential that was first recorded from the frog (Sickel and Crescitelli, 1967). It has since been described in other amphibians (tadpole: Crescitelli, 1970; mudpuppy: C. J. Karwoski, unpublished observations), and it may well exist in other vertebrates, since delayed-OFF neuronal responses have been recorded in cat (Steinberg, 1969). The *e*-wave can be recorded transretinally only on occasion (Newman and Lettvin, 1978), but it is regularly observed with intraretinal recordings as a relatively rapid, negative dip, that is superimposed on the slower *c*-wave/slow-PIII complex. The response is distinguished by its long latency following light offset, which can vary from 2 to over 60 sec (Newman and Lettvin, 1978).

Since the *e*-wave appears only in the dark-adapted retina, it is believed to be related to a set of retinal events (shown in schematic form in Fig. 1) known to be initiated by rod activity in response to high levels of illumination. Specifically, as flash intensity is increased, rod responses become larger, but eventually plateau in amplitude, or "saturate". Further increases in flash intensity lengthen the duration of this saturated rod response (e.g. Toyoda *et al.*, 1970; Normann and Werblin, 1974; Cervetto *et al.*, 1977). This "rod aftereffect" is thought to generate prolonged responses in horizontal cells (Steinberg, 1969), as well as in the rest of the retinal circuitry, and to give rise to prolonged spike discharges in ON ganglion cells (Steinberg, 1969; Karwoski and Burkhardt, 1976). Delayed OFF-responses in OFF and ON/OFF ganglion cells (Pickering and Varju, 1967; Steinberg, 1969; Karwoski and Burkhardt, 1976; Zeise and Hamdorf, 1983; Olsen *et al.*, 1986) and the *e*-wave (Newman and Lettvin, 1978) are triggered when the rod aftereffect begins to decay. Since the duration of the rod aftereffect lengthens with increasing flash intensity, delayed OFF-responses (including the *e*-wave) exhibit the peculiar property that their latency increases as flash intensity is increased (Crescitelli and Sickel, 1968).

The exact relationship between neuronal OFF-responses and the *e*-wave is uncertain, and various hypotheses relating these events have appeared over the years. Most recently, theories of *e*-wave generation have emphasized its close relation to the delayed OFF-responses in the proximal retina (Newman, 1977; Newman and Lettvin, 1978; Tomita *et al.*, 1978). The present

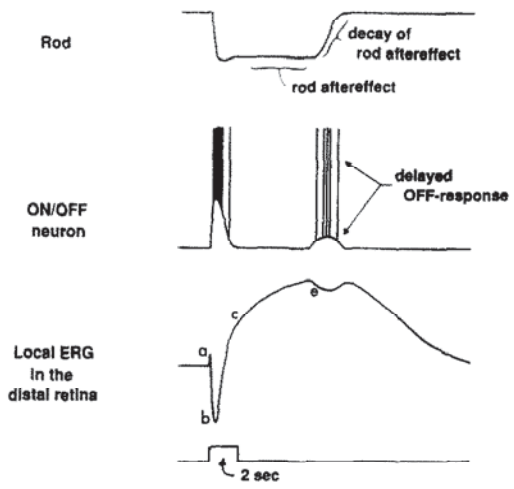

Fig. 1. Schematic of retinal responses evoked by high intensity illumination to the rod system. Top: intracellular rod response shows rod aftereffect and delayed decay of the aftereffect. Middle: ON/OFF-neuron shows ON-response, and delayed OFF-response, both of which are thought to be triggered by changes in the rod potential. Bottom: intraretinal ERG, showing *a*-, *b*-, *c*- and *e*-waves. Note that the *e*-wave occurs at the same time as the delayed-OFF ganglion cell discharge.

paper describes a number of observations that support the idea that the *e*-wave arises from delayed OFF activity in the proximal retina, and it specifically suggests that the *e*-wave results from Muller cell currents induced by K^+ released in the proximal retina.

METHODS

Most of the experiments were performed at the University of California San Francisco, CA, on medium to large *Rana pipiens* and *Rana catesbeiana*. Usually eyecups were dissected and superfused at room temperature (~23°C) with an amphibian Ringers solution similar to that of Miller and Steinberg (1977), but with K^+ concentration increased to 2.7 mM. A few experiments were done on isolated retinas that were mounted receptor-side up and superfused with the same solution. It was our impression that responses from isolated retinas deteriorated more quickly than those from eyecups, but no important differences regarding results reported in this paper were noted. In some experiments, 1 μM tetrodotoxin (TTX) was added to the superfusate. In these experiments, control (predrug) responses were stable for at least 15 min prior to TTX application, TTX responses were measured 10–20 min after drug application began, and effects were largely reversible 40–60 min after TTX application ended.

Recordings of light-evoked field potentials (ΔV_0) and of potentials related to the extracellular K^+ concentration (ΔV_K) were obtained with double-barreled K^+ selective microelectrodes fabricated via methods similar to those described by Steinberg *et al.* (1980). Corning resin 477317 was injected into the tip of the active barrel, and both the active and reference barrels were then backfilled with 120 mM NaCl and 2.7 mM KCl. The tips were beveled and had a diameter of 1–2 μm across the unbeveled portion of the tip. The reference electrode for the recordings of ΔV_0 was a salt bridge in contact with the sclera at the back of the eye. Signals were recorded with an amplifier (FD 223 Electrometer, World Precision Instruments) that had no negative capacitance feature, and thus the rise-time (time to 63% of final value) of the active barrel was about 250 msec. In most experiments, the transretinal ERG was also recorded between salt-bridges located at the sclera and within the superfusate flowing over the eyecup.

The optical system used a light source (Halogen Bellaphot No. 64625,, operated at 5 V) that produced nearly white light. The duration, intensity, and diameter of each flash could be controlled. Usually, a duration of 4–8 sec was used, since this allowed unequivocal discrimination of ON-responses from regular (fast) OFF-responses, and since it also generated clear delayed-OFF activity (*e*-wave). The maximum light output was measured in $\mu W/cm^2$ and converted to a retinal illumination of 5×10^7 equivalent quanta [(507 nm) $\mu m^{-2} \cdot sec^{-1}$]. In this paper, this value is equated to a $\log(I)$ of 9.8, following the convention of Newman and Lettvin (1978), where a 100 msec flash at $\log(I) = 0$ produced a threshold ERG response in dark-adapted eyes. Unless otherwise indicated, light flashes of $\log(I) = 6.8$ were used in this study, since this value elicited *e*-waves of near maximum amplitude. Surround antagonism was assessed by using small (0.3 mm) and large (6.0 mm) dia. spots. An interstimulus interval of 1 min was usually used.

Responses were fed on-line to a d.c. chart recorder (Brush, Mark 240) that had a 3 dB cut-off set at 100 Hz. Some of the responses shown in this paper required retouching prior to photography.

Current source density (CSD) analysis

CSD experiments were performed at the Massachusetts Institute of Technology, Cambridge,

MA, on ΔV_0 obtained in *Rana pipiens*. Eyecups were maintained in a moist atmosphere at 95% O_2/5% CO_2 at 15°C. Nearly white light flashes of 100 msec duration illuminated the retina diffusely at a log(I) of between 5.7 and 6.4 and with an interstimulus interval of 2–3 min. Responses were recorded with single barrel electrodes (~3 μm tip dia.) filled with amphibian Ringer (Newman and Lettvin, 1978) and were referenced to a second electrode in the vitreous. The relatively large tip diameter of the intraretinal electrode may have locally damaged the retina along the electrode track. This region of damage may have somewhat reduced the spatial resolution of the CSD plots. However, when retinal currents were calculated, intraretinal voltage measurements were corrected for variations in the local resistivity of the retina. This reduced possible errors in computing intraretinal currents, because the current flowing through a damaged region was calculated from resistance measurements made on the same damaged region. Other experimental details can be found in Newman (1977) and Newman and Lettvin (1978).

The methods used to compute CSD profiles are described in detail in Newman (1980). Briefly, intraretinal ERG and resistance measurements were made at 8 μm intervals during the withdrawal of an electrode from the pigment epithelium. The electrode was first advanced through the retina and was judged to have penetrated the pigment epithelium when there was a large increase in the measured intraretinal resistance. Intraretinal resistance measurements were made by passing constant current pulses (10 μA) across the eyecup and by measuring the voltage drop between the intraretinal electrode and a vitreal reference electrode.

Since the *e*-wave was superimposed on the *c*-wave, it was necessary to estimate the time-course of the *c*-wave in order to measure *e*-wave amplitde. This was accomplished by hand-drawing a smooth curve to connect portions of the *c*-wave that had been interrupted by the *e*-wave. The reconstructed portion of the *c*-wave served as a baseline for measuring the peak amplitude of the *e*-wave. We believe this procedure was accurate, since the *e*-wave appears to have a relatively abrupt beginning and end. In preliminary experiments, the baseline was also determined by fitting those portions of the *c*-wave occurring before and after the *e*-wave to a fourth-order polynomial by a least-squares procedure. The *e*-wave amplitudes obtained using this computer-fitted method did not differ significantly from those obtained using the hand-drawn baselines. The latter method was simpler and was thus used in the present report. Other aspects of the computation of CSD profiles were identical to those presented elsewhere (Newman, 1979; 1980).

The CSD profiles of the *e*-wave shown in this paper represent those calculated at the peak of the response. However, the rising and falling phases of the *e*-wave recorded at different retinal depths all had similar time courses, which indicates that the spatial distribution of the *e*-wave CSD did not significantly shift during the course of the response.

RESULTS

e-Wave and $\Delta[K^+]_0$

The first set of results examines the behavior of the *e*-wave as a function of recording depths, and of stimulus intensity and diameter. In addition, light-evoked $\Delta[K^+]_0$ was measured simultaneously with ΔV_0 in many of these experiments. This was to test the possibility that the *e*-wave is generated by a mechanism dependent on a K-increase in the proximal retina. If such a mechanism exists, then a delayed OFF K-increase should be measurable, and it should have features (e.g. time course, intensity-dependence) consistent with those of the *e*-wave.

Depth-dependence

The intraretinally-recorded *e*-wave is a negative-going potential, and its amplitude varies characteristically with retinal depth. The depth profile of the response also depends on stimulus dia. With a 6.0 mm spot, the *e*-wave can be detected at all intraretinal depths. This is seen in Fig. 2 (left column), which shows field potentials (ΔV_0) evoked during withdrawal of the electrode from 90% retinal depth (near the pigment epithelium) to the vitreous humor just proximal to the retinal surface (S). In Fig. 2, the *e*-wave occurs about 6 sec after stimulus offset. Though recorded well at all intraretinal depths, it has maximum amplitude in the proximal retina at 20–30% retinal depth (see also Newman, 1977), and it cannot be recorded transretinally (S).

With a 0.3 mm stimulus, *e*-wave amplitude also is maximum in the proximal retina, but it is now more localized in depth (Fig. 3, left column). In this depth profile, the *e*-wave has

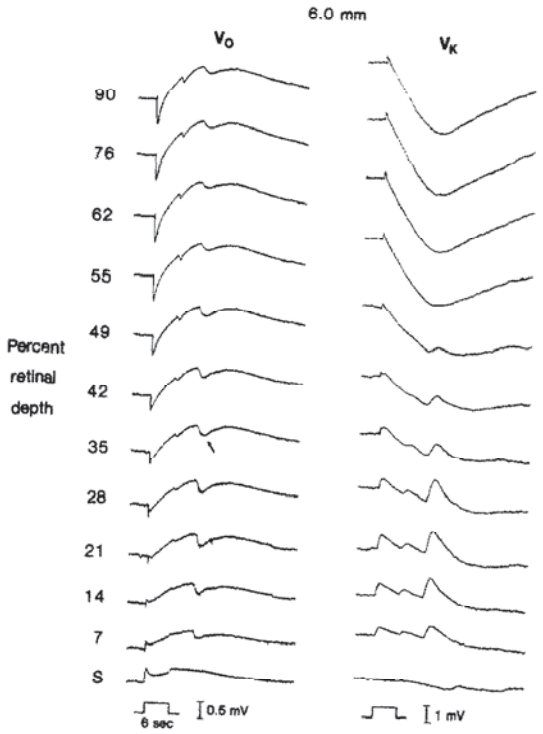

Fig. 2. Depth series from an eyecup of light-evoked field potentials (V_0, plotted positive-up), and of V_K to large spot (6.0 mm) stimuli. Recordings were made simultaneously with double-barreled K-ISMs. Depth 90% is near the pigment epithelium, and depth *S* is at the proximal surface of the retina, near the inner limiting membrane. The 1 mV V_K calibration represents an increase in $[K^+]_0$ of ~0.19 mM. Arrow at 35% retinal depth points to *e*-wave of V_0.

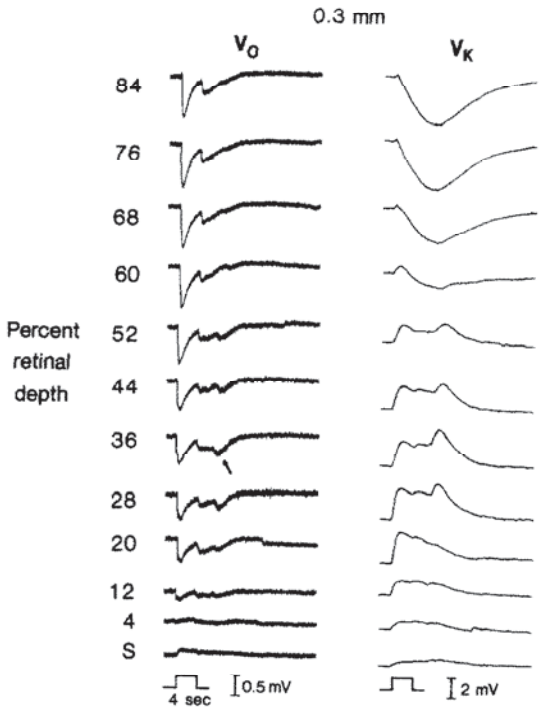

Fig. 3. Depth series of V_0 and V_K to small spot (0.3 mm) stimulation. The 2.0 mM V_K calibration represents an increase in $[K^+]_0$ of ~0.39 mM. Other details as in Fig. 1.

maximum amplitude in the proximal retina (at ~28–36% retinal depth), but it is difficult to observe in the distal half of the retina and near the retinal surface.

Light-evoked ΔV_K exhibited a depth profile generally similar to what has been described previously (Oakley and Green, 1976; Karwoski and Proenza, 1978): a K-decrease in the distal retina, and separate increases at light onset and offset in the proximal retina (right columns of Figs 2 and 3). However, a feature in these responses not described elsewhere is the delayed-OFF K-responses occurring in the proximal retina several seconds after light offset and after the well-known fast-OFF K-increase. In both Figs 2 and 3, the delayed-OFF K-response has several features consistent with it generating the *e*-wave: (1) it is a K-*increase*; (2) it is only seen in the proximal half of the retina, and it has maximum amplitude at the same depths at which *e*-wave amplitude is maximum; and (3) its latency and time-course are similar to the *e*-wave.

Depths of maximum amplitudes of the *e*-wave and the K-increase are quantified in Table 1 (column 1). Here, the depth at which the ON K-increase to the 0.3 mm spot was maximum is normalized to 0 μm. This depth is known to be in the proximal half of the inner plexiform layer (Karwoski *et al.*, 1985). The depths at which the other responses are maximum are listed relative to this depth, such that a positive value represents a more distal location. For both the 6.0 and 0.3 mm spots, the fast-OFF K-increase and the delayed-OFF K-increase peak about 17 μm distal to the ON K-increase. This laminar separation between the ON and OFF K-increase has been previously reported (Karwoski *et al.*, 1978, 1985). The present result suggests that the delayed-OFF K-increase is also generated in the distal half of the inner plexiform layer.

The *e*-wave also is maximum in the distal portion of the inner plexiform layer (Table 1). Thus, the *e*-wave and delayed-OFF K-increase are closely related in depth.

Intensity-dependence

Intensity series of field potentials recorded in the proximal retina are shown in Fig. 4 (left column). Responses to a 0.3 mm spot (Fig. 4A) show transient negativities at light onset and

Table 1. Amplitudes and depths of maximum amplitude[a] of *e*-wave and K-increase to 0.3 and 6.0 mm dia. light flashes

Diameter	Response	Depth of maximum amplitude $\bar{X} \pm$ SEM (μm)	Amplitude $\bar{X} \pm$ SEM
6.0 mm	*e*-wave	17 ± 7 ($N = 7$)	0.22 ± 0.03 mV ($N = 18$)
	ON K-increase	1 ± 0 ($N = 9$)	0.35 ± 0.04 mM ($N = 18$)
	OFF K-increase	17 ± 5 ($N = 9$)	0.16 ± 0.02 mM ($N = 18$)
	Delayed-OFF K-increase	18 ± 7 ($N = 8$)	0.26 ± 0.05 mM ($N = 18$)
0.3 mm	*e*-wave	8 ± 6 ($N = 7$)	0.26 ± 0.03 mV ($N = 14$)
	ON K-increase	0 ± 0 ($N = 7$)	0.68 ± 0.05 mM ($N = 15$)
	OFF K-increase	16 ± 8 ($N = 7$)	0.22 ± 0.06 mM ($N = 15$)
	Delayed-OFF K-increase	16 ± 7 ($N = 7$)	0.26 ± 0.06 mM ($N = 15$)

[a]Depth of maximum amplitude given as microns distal to the depth (proximal inner plexiform layer) at which the ON K-increase is maximum for the 0.3 mm spot.

offset, which have a threshold at about $I = 1.8$ and are of larger, but of relatively constant, amplitude over the next 6 log units. These transients consist of the proximal negative response (PNR) and *M*-wave (Burkhardt, 1970; Karwoski and Proenza, 1977). At $I = 4.8$, the OFF-response broadens, and at $I = 5.8$ and 6.8, distinct *e*-waves are apparent. As reported previously, *e*-wave latency increases with intensity, and its amplitude decreases at the highest intensities (Crescitelli and Sickel, 1968; Tomita *et al.*, 1978). An intensity of 6.8 was primarily used in the present study, since this reliably evoked a large and distinct *e*-wave.

The intensity series to the 6.0 mm stimulus (recorded from the same retina) is shown in Fig. 4B. The field potential at light onset and at offset is complex, but an *e*-wave is visible, particularly at $I = 5.8$ and 6.8. For both 0.3 and 6.0 mm stimuli, intensities in this range were optimum for eliciting a relatively large and distinct *e*-wave. For the transretinal response (ERG, in Fig. 4), an *e*-wave is not apparent at any stimulus intensity.

The delayed-OFF K-increase also paralleled the *e*-wave as a function of stimulus intensity. This can be seen for both the 0.3 and 6.0 mm stimuli in Fig. 4, where the delayed-OFF K-increase (middle column) and the *e*-wave (left column) appear together at $I = 5.8$, have increased in latency at 6.8, and at $I = 7.8$ have further increased in latency and decreased in amplitude.

Surround antagonism

The amplitudes of the *e*-wave and the delayed-OFF K-increase to the small (0.3 mm) and large (6.0 mm) dia. stimuli were measured, and the strength of surround effects for each response was expressed as a "surround effects ratio" (SER) defined as log [(response amplitude to 6.0 mm)/(response amplitude to 0.3 mm)]. With this measure, values less than zero indicate surround antagonism, whereas values greater than zero indicate spatial summation.

The mean *e*-wave SER is nearly zero, and the distribution of these values can be read along the abscissa of Fig. 5 (SER-e). These values show considerable variation, with 4 preparations showing clear surround antagonism (SER-e < -0.15), 4 showing clear response summation (SER-e $> +0.15$), and 6 showing little effect of spot diameter on response amplitude (SER-e $= 0 \pm 0.1$). (An example of an *e*-wave exhibiting surround antagonism is shown in Fig. 4—compare *e*-waves at $I = 5.8$ and 6.8 to 0.3 and 6.0 mm spots; an example of an *e*-wave showing neither surround antagonism nor summation is in Fig. 22 of Newman, 1977). Surround effects in the delayed-OFF K-increase were also variable (Fig. 5, SER-K along the ordinate), with some preparations exhibiting strong surround antagonism (e.g. Fig. 4), and others showing response summation. The reason for the variability in SERs is not clear: SERs were stable over several hours within a preparation, they were not a function of frog species or

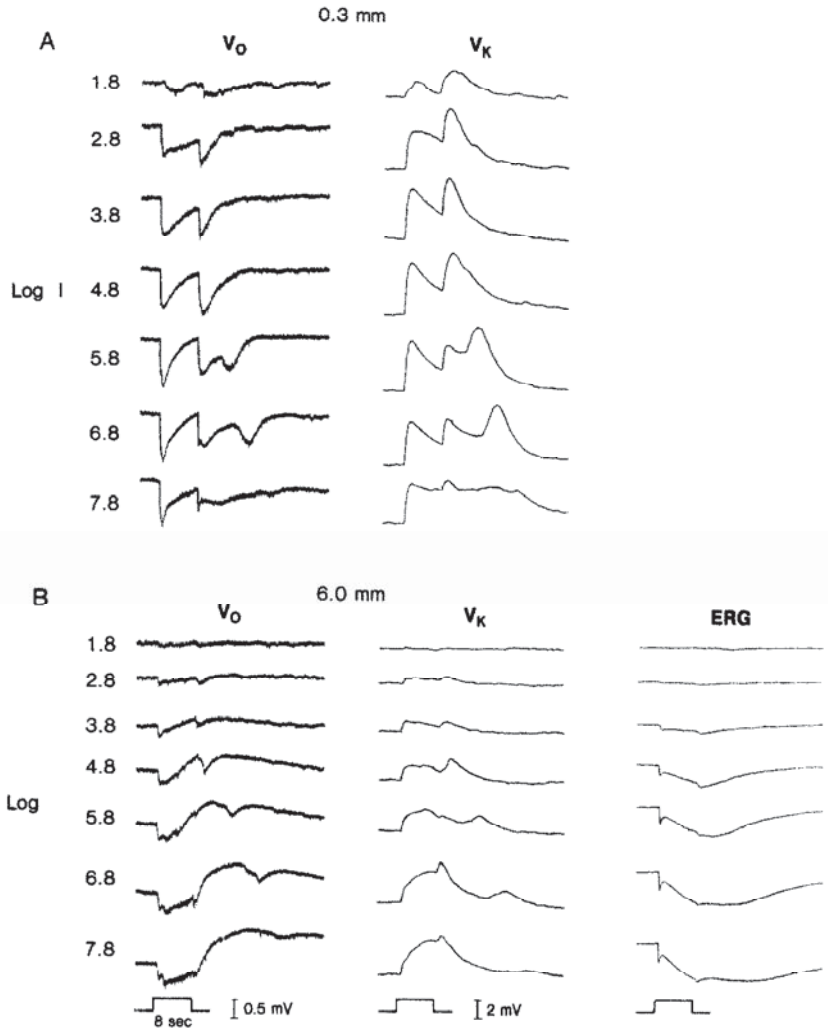

Fig. 4. Responses to 0.3 (A) and 6.0 mm (B) stimuli of increasing intensity. Recordings of V_0 and V_K were made in the inner plexiform layer. ERG traces, recorded transretinally and plotted negative-up, are only shown for the 6.0 mm stimuli. The ERG responses to 0.3 mm stimuli were negligible in amplitude. All recordings are from the same preparation, and recordings in each row (A and B) were made simultaneously. The 2.0 mV calibration for V_K represents an increase in $[K^+]_0$ of ~0.39 mM.

of background light level within the scotopic range, and they could not be reliably altered by changes in test flash intensity. Although all of our recordings were made in approximately the posterior third of the eyecup (a region within about 1.5 mm of the optic disc and which on one side encompasses part of the area centralis), we did not control for the exact recording site within this region, and it is possible that this could explain some of the variability in SER-e.

Regardless of the reason for the variability in surround strengths, we view it as important that SER-e and SER-K within any one preparation were highly correlated (Fig. 5). Here, the solid line shows the linear regression line of best fit, and the Pearson correlation coefficient (r) was 0.89 ($P < 0.00001$). Thus, although surround effects in the e-wave and in the delayed-OFF K-increase vary across preparations, the surround strength of these responses within a preparation are very similar. This correlation is further supportive of a relationship between the delayed-OFF K-increase and the e-wave.

The lack of reliable surround antagonism in the e-wave and in the delayed-OFF K-increase was somewhat surprising, since it is well-known that other responses of the proximal retina (for example, the PNR/M-wave and the IPL K-increase at light onset) generally exhibit surround antagonism. We also calculated SERs for the fast-OFF K-increase of these same dark-adapted retinas and obtained similar results—

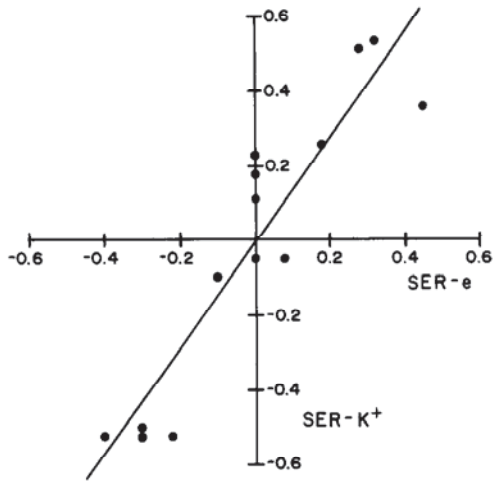

Fig. 5. Plot of surround effects calculated from simultaneous recordings of *e*-wave and delayed-OFF K-increases in 14 preparations. The surround effects ratio (SER) is defined as log [(response amplitude to 6.0 mm)/(response amplitude to 0.3 mm)].

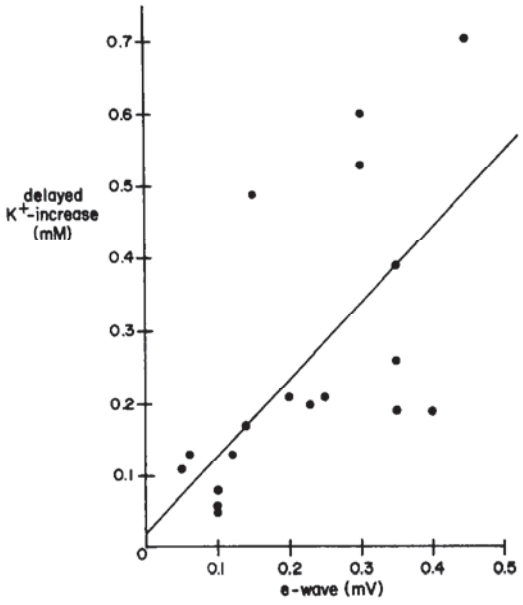

Fig. 6. Plot of amplitudes of simultaneously-recorded *e*-wave and delayed-OFF K-increase from the inner plexiform layer. Spot diameter: 6.0 mm.

half of the retinas showed surround antagonism, while half showed response summation. In contrast, in 15 light-adapted retinas, the fast-OFF K-increase exhibited surround antagonism in every case, although the degree of surround antagonism was less than in the ON K-increase. Thus, it appears that in the dark-adapted retina, proximally-recorded OFF-responses do not exhibit surround antagonism as reliably as in the light-adapted retina. Therefore, the failure to consistently observe surround antagonism in the *e*-wave does not argue against it having a proximal origin.

Amplitude

Table 1 shows amplitudes ($\bar{X} \pm$ SEM) of the *e*-wave recorded at the best depths and to both the 6.0 and 0.3 mm spots. Even when optimum stimulus intensities are used, the *e*-wave is a relatively small response, rarely exceeding 0.4 mV. In contrast, the PNR/*M*-wave and negative-going *b*-wave usually exceeded 1.0, and sometimes 2.0 mV.

The amplitudes of the K-increases are also quantified in Table 1. As previously reported (Karwoski *et al.*, 1978), the ON K-increase to the 0.3 mm spot is relatively large, averaging almost 0.7 mM. This response reliably showed surround antagonism, since its amplitude was only half as great to the 6.0 mm spot. In contrast, both the fast-OFF and the delayed-OFF K-increases were smaller in amplitude, averaging less than 0.3 mM, and (as described above) neither response reliably showed strong surround antagonism. Although the *e*-wave and delayed-OFF K-increase exhibited considerable variability in amplitude across preparations, their amplitudes within a given preparation correlated fairly well: in Fig. 6, the amplitude of the *e*-wave (in mV) is plotted against the K-increase (in mM), along with the linear regression line of best fit. The Pearson r was 0.66 ($P < 0.002$), thus providing additional support for a relationship between the K-increase and the *e*-wave.

Role of action potentials

In a variety of neural tissues, TTX has been shown to selectively block the Na^+ channels that mediate action potentials (see, e.g. Hille, 1984, for a review). In the vertebrate retina, TTX blocks the somatic and dendritic spikes of amacrine cells (Miller and Dacheux, 1976) and somatic spikes of ganglion cells (Newman, 1977), but has no reported effects on the post-synaptic potentials of bipolar (Maple and Werblin, 1986) or amacrine (Miller and Dacheux, 1976) cells, or on Muller cell channels (Newman, 1985b). Since the *e*-wave may be generated by a mechanism dependent on the delayed-OFF K-increase, and sinced delayed-OFF spike activity should be associated with K^+ release into the extracellular space of the proximal retina, the effects of TTX on the *e*-wave and on the K-increases were examined.

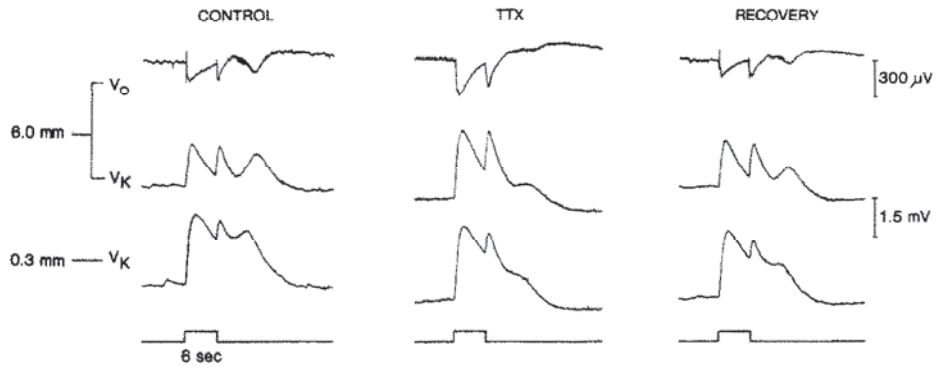

Fig. 7. Effects of 1.0 μM TTX on V_K and V_0 simultaneously recorded from the inner plexiform layer to a 6.0 mm spot. The effect of TTX on V_K to a 0.3 mm spot is shown in the bottom row. Responses labelled "TTX" were obtained 7 min after application of TTX began, and "RECOVERY" responses were obtained 28 min after TTX superfusate was switched back to normal Ringer.

TTX (1 μM) was applied to 7 retinas, and the results are typified by the responses shown in Fig. 7: TTX substantially decreased the amplitudes of both the *e*-wave and delayed-OFF K-increase. The *e*-wave was reduced to 55 ± 9% ($\bar{X} \pm$ SEM; $N = 11$) of its control value by TTX. The delayed-OFF K-increase was reduced to 47 ± 13% ($N = 7$) of its control value. These effects developed within a few minutes of switching to TTX. Upon switching back to control Ringer, responses started to recover at about 15 min, showed appreciable recovery at 30 min, but did not usually fully recover even at 1 hr. These results were obtained regardless of whether the proximal surface of the retina was superfused (in the eyecup) or whether superfusion was over the rod outer segments of the isolated retina.

In Fig. 7, it could be argued that with 6.0 mm spot stimulation, TTX results in enhanced ON and fast-OFF K-increases, which then depresses the delayed-OFF K-increase simply because the neurons are less sensitive following these enhanced responses. Results with the K-increase to 0.3 mm (Fig. 7, bottom row) argue against this interpretation, since TTX had little effect on the ON and fast-OFF K-increases, yet still depressed the delayed-OFF K-increase.

TTX regularly increased the ON K-increase to 6.0 mm spots. However, other responses that were examined during TTX application (K-decrease in the subretinal space, *b*-wave, *c*-wave, ON K-increase and ON PNR/*M*-wave to 0.3 mm, OFF PNR/*M*-wave, and the fast-OFF K-increases to the 6.0 and 0.3 mm spots) showed erratic or small changes in amplitude. In summary, TTX substantially reduced delayed-OFF activity in the proximal retina, without greatly affecting ON or fast-OFF retinal responses.

Current source-density analysis

The close correlation between the *e-wave* and the delayed-OFF K-increase recorded in the inner plexiform layer suggests that the *e*-wave may be generated by this K-increase. The ERG *b-wave* is believed to be generated, in large part, by separate K-increases in the inner and outer plexiform layers, with these K-increases leading to influx of K^+ into Muller cells (the principal glial cells of the retina) and to the establishment of a radial current flow within the retina (e.g. Newman and Odette, 1984). To assess whether a similar mechanism might also underlie *e*-wave generation, CSD analysis was used to localize the sources and sinks of this response.

Four CSD profiles were obtained from penetrations in 3 frog eyecups, and these are shown in Fig. 8. As illustrated in this figure, the *e*-wave is generated principally by a current sink in the proximal retina and by a current source at the vitreal surface of the retina (0% retinal depth). A secondary current source occurs distal to the current sink in some instances (Fig. 8A and D). The position of the current sink corresponds approximately to a location within the inner plexiform layer (Newman, 1980). Although there is significant variation among these four plots, the main features—a current sink near the inner plexiform layer and a large current source at the retinal surface—were present in all of the *e*-wave CSD profiles.

b-Wave CSD distributions were calculated from the same intraretinal records as were the *e*-wave distributions. One *b*-wave CSD profile, along with the *e*-wave profile recorded during

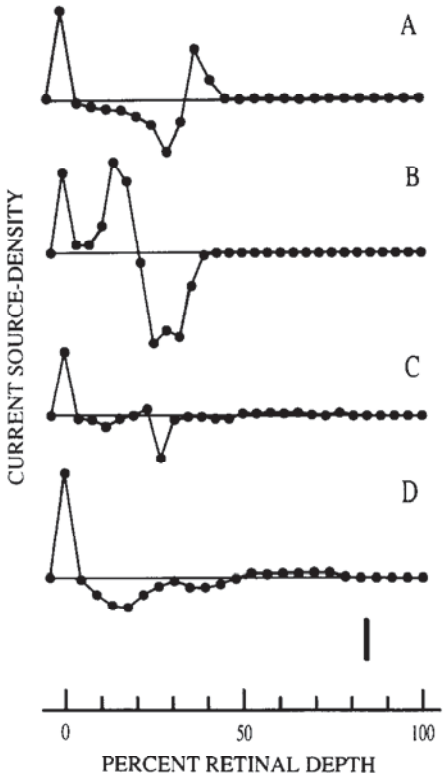

Fig. 8. Four CSD profiles of the *e*-wave recorded from the dark-adapted frog eyecup. Light stimulus: 100 msec flash; $\log(I) = 6.45$, 6.0, 6.0, and 5.7 in A–D, respectively. Scale bar = 2 mA · cm^{-3}.

the same penetration, is illustrated in Fig. 9. The *b*-wave plot is similar to those published previously (Newman, 1980), but differs from the *e*-wave plots in one important feature: whereas the *e*-wave was generated principally by a current sink in the proximal retina (proximal sink), the *b*-wave arose from one sink in the proximal retina and from a second sink in the distal retina (distal sink) (Fig. 9). There was never an indication of this second sink in the CSD records of the *e*-wave (Fig. 8). Thus, the CSD experiments confirm that the *e*-wave is primarily a phenomenon of the proximal retina.

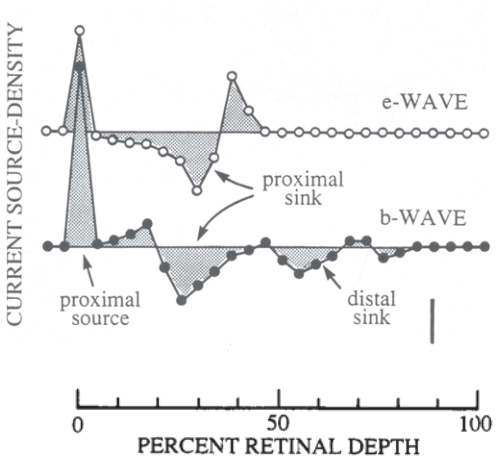

Fig. 9. Current source-density distributions of the ERG *e*-wave and *b*-wave recorded from a dark-adapted frog eyecup. The paired *e*-wave/*b*-wave plot was computed from the same intraretinal records. The *e*-wave profile is the same as shown in Fig. 8A. Light stimulus, 100 msec flsh; $\log(I) = 6.45$. Scale bar: 2 mA · cm^{-3}.

DISCUSSION

The problem of determining whether a field potential in the nervous system is of direct neuronal origin or of glial origin is well-known and has received much attention in the analysis of the components of the electroretinogram. In the present paper, numerous observations indicate that the *e*-wave is generated by cells of the proximal retina. However, the specific cellular origin (neural or glial) of the *e*-wave is a knottier issue. For example, neurons in the proximal retina show delayed-OFF activity (graded and action potentials), and the neuronal currents associated with this activity could directly generate the *e*-wave. Alternatively, the delayed-OFF K-increase produced by this neuronal activity could lead to localized influx of K^+ into Muller cells, with the resultant currents giving rise to the *e*-wave.

In support of the latter "Muller cell hypothesis" are our CSD results, which show that the *e*-wave is generated principally by a current sink in the proximal retina, a large current source sharply localized at the retinal surface, and, sometimes, a weaker source in the mid-retina. Such a source-sink profile is suggestive of a Muller cell origin for a field potential (Faber, 1969; Newman, 1980). In the case of the *e*-wave, since its current sink and the delayed-OFF K-increase are both centered at about the same retinal level (inner plexiform layer), the current sink is likely due to K^+ influx into Muller cells at that site. A large fraction of this K^+ current would flow out from Muller cell endfeet, which have much higher K^+ conductance than other cell regions (Newman, 1985a). The K^+ efflux from Muller cell endfeet, which lie against the inner limiting membrane, would generate the large current source seen at the retinal surface (Fig. 9: proximal source). The remainder of the current, which would flow out from the distal portions of Muller cells, would give rise to the secondary current source seen in some of the CSD plots. The return current flow through extracellular space (from the sources to the sink)

would then generate the negative intraretinal *e*-wave.

This proposed mechanism of *e*-wave generation has similarities to that believed to underlie generation of the *M*-wave (Karwoski and Proenza, 1977). Additionally, the *e*- and *M*-waves are both recorded maximally in the proximal retina, but neither is normally observed in transretinal recordings. Since both the *e*-wave and delayed-OFF K-increase are maximum in the distal half of the inner plexiform layer, at the same level as the OFF PNR/*M*-wave and fast-OFF K-increase (Karwoski *et al.*, 1978), it is possible that the *e*-wave should simply be considered the scotopic *M*-wave OFF-response. On the other hand, Tomita *et al.* (1978) have argued that the *e*-wave is the scotopic *d*-wave. The exact relationship between the *e*-wave, scotopic *d*-wave, and scotopic *M*-wave has still to be worked out.

Tetrodotoxin is well-known to selectively block action potentials, while leaving graded potentials unaffected. Moreover, a voltage-clamp study of dissociated salamander Muller cells has shown that TTX does not affect Muller cell membrane conductance (Newman, 1985b). Thus, the finding that the *e*-wave and the delayed-OFF K-increase remain after TTX treatment indicates that graded potentials in the inner plexiform layer are associated with K^+ release that directly contributes to current flow through Muller cells. However, since the *e*-wave and delayed-OFF K-increase are diminished $\sim 50\%$ by TTX, action potentials also play an important role in *e*-wave generation. The nature of this role is uncertain: potassium release by amacrine and ganglion cell spikes might directly contribute to current flow through Muller cells. Alternatively, it may prove that amacrine cell spikes, which are blocked by TTX (Miller and Dacheux, 1976), are important for the generation of delayed-OFF graded potentials, in other amacrine cells and in ganglion cells, which in turn, produce K-increases. Regardless of the exact mechanism of TTX action, our results reinforce the finding that activity in the proximal retina leads to the generation of the *e*-wave, and also demonstrate that action potentials are involved in the events leading to *e*-wave generation.

The delayed-OFF and fast-OFF responses (ΔV_0 and $\Delta[K^+]_0$) of the proximal retina differed in their sensitivity to TTX (Fig. 8). The delayed-OFF responses were depressed $\sim 50\%$ by TTX, whereas the fast-OFF responses were unaffected, or even increased. This suggests a difference in the relative role of action potentials in generating these responses. The mechanism underlying this difference is unknown, but might have to do with the time courses of photoreceptor responses. For example, delayed-OFF responses of the proximal retina are initiated by a gradual event, the decay of the rod aftereffect (Fig. 1). When the proximal retina is driven by such a slow signal, action potentials may play a major role in the amplification of responses, and/or in the release of K^+. Fast-OFF responses of the proximal retina, however, are triggered by more abrupt OFF-responses in the photoreceptors. Under these circumstances, action potentials may be relatively less important in the propagation of responses through the proximal retina, and/or in the release of K^+.

Acknowledgements—This research was supported in part by NIH grants EY-03526 to Luis M. Proenza, EY-01429 to Roy H. Steinberg, EY-04077 to Eric A. Newman, and EY-00090 to Jerome Y. Lettvin. We thank Drs Roy H. Steinberg, Joe Immel, and Laura J. Frishman for helpful discussion and for comments on an earlier version of the manuscript.

REFERENCES

Burkhardt D. A. (1970) Proximal negative response of frog retina. *J. Neurophysiol.* **33,** 405–420.

Cervetto L., Pasino E. and Torre V. (1977) Electrical responses of rods in the retina of *Bufo marinus*. *J. Physiol., Lond.* **267,** 17–51.

Crescitelli F. (1970) The *e*-wave and inhibition in the developing retina of the frog. *Vision Res.* **10,** 1077–1091.

Crescitelli F. and Sickel E. (1968) Delayed OFF responses from the isolated frog retina. *Vision Res.* **8,** 801–16.

Faber D. S. (1969) Analysis of the slow trans-retinal potentials in response to light (Ph.D. Thesis). State University of New York at Buffalo.

Hille B. (1984) *Ionic Channels of Excitable Cells*. Sinauer, Sunderland, Mass.

Karwoski C. J. and Burkhardt D. A. (1976) Ganglion cell responses of the mudpuppy retina to flashing and moving stimuli. *Vision Res.* **16,** 1483–1495.

Karwoski C. J. and Proenza L. M. (1977) Relationship between Muller cell responses, a local transretinal potential, and potassium flux. *J. Neurophysiol.* **40,** 244–259.

Karwoski C. J. and Proenza L. M. (1978) Light-evoked changes in potassium concentration in mudpuppy retina. *Brain Res.* **142,** 515–530.

Karwoski C. J. and Proenza L. M. (1980) Transient adaptive and sensitizing effects in the retina of *Necturus*. *J. gen. Physiol.* **76,** 479–497.

Karwoski C. J., Criswell M. H. and Proenza L. M. (1978) Laminar separation of light-evoked K^+-flux and field potentials in frog retina. *Invest. Ophthal. visual Sci.* **17,** 678–682.

Karwoski C. J., Newman E. A., Shimazaki H. and Proenza L. M. (1985) Light-evoked increases in extracellular K^+

in the plexiform layers of amphibian retinas. *J. gen. Physiol.* **86,** 189–213.

Maple B. R. and Werblin F. S. (1986) Inhibitory feedback to bipolar cells in the tiger salamander retina. *Soc. Neurosci. Abstr.* **12,** 634.

Miller R. F. and Dacheux R. (1976) Dendritic and somatic spikes in mudpuppy amacrine cells: identification and TTX sensitivity. *Brain Res.* **104,** 157–162.

Miller S. S. and Steinberg R. H. (1977) Passive ionic properties of frog retinal pigment epithelium. *J. Membrane Biol.* **36,** 337–372.

Newman E. A. (1977) The *e*-wave of the frog retina: its origin and relation to the delayed ganglion cell response and the prolonged rod response (Ph.D. Thesis). MIT, Cambridge, MA.

Newman E. A. (1979) *b*-wave currents in the frog retina. *Vision Res.* **19,** 227–234.

Newman E. A. (1980) Current source-density analysis of the *b*-wave of frog retina. *J. Neurophysiol.* **43,** 1355–1366.

Newman E. A. (1985a) Membrane physiology of retinal glial (Muller) cells. *J. Neurosci.* **5,** 2225–2239.

Newman E. A. (1985b) Voltage-dependent calcium and potassium channels in retinal glial cells. *Nature, Lond.* **317,** 809–811.

Newman E. A. and Lettvin J. Y. (1978) Relation of the *e*-wave to ganglion cell activity and rod responses in the frog. *Vision Res.* **18,** 1181–1188.

Newman E. A. and Odette L. L. (1984) Model of electroretinogram *b*-wave generation: a test of the K^+ hypothesis. *J. Neurophysiol.* **51,** 164–182.

Normann R. A. and Werblin F. S. (1974) Control of retinal sensitivity: I. light and dark adaptation of vertebrate rods and cones. *J. gen. Physiol.* **63,** 37–61.

Oakley B. and Green D. G. (1976) Correlation of light-induced changes in retinal extracellular potassium concentration with *c*-wave of the electroretinogram. *J. Neurophysiol.* **39,** 1117–1133.

Olsen B. T., Schneider T. and Zrenner E. (1986) Characteristics of rod driven off-responses in cat ganglion cells. *Vision Res.* **26,** 835–845.

Pickering S. G. and Varju D. (1967) Ganglion cells in the frog retina: inhibitory receptive field and long-latency response. *Nature, Lond.* **215,** 545.

Sickel W. and Crescitelli F. (1967) Delayed electrical responses from the isolated frog retina. *Pflügers Arch. ges. Physiol.* **297,** 266–269.

Steinberg R. H. (1969) High-intensity effects on slow potentials and ganglion cell activity in the area centralis of cat retina. *Vision Res.* **9,** 333–350.

Steinberg R. H., Oakley B. and Niemeyer G. (1980) Light-evoked changes in $[K^+]_o$ in retina of intact cat eye. *J. Neurophysiol.* **44,** 897–921.

Tomita T., Matsuura T., Fujimoto M. and Miller W. H. (1978) The electroretinographic *c*- and *c*-waves with special reference to the receptor potential. *Proc. 16th ISCEV Symp., Morioka,* 15–25.

Toyoda J., Hashimoto H., Anno H. and Tomita T. (1970) The rod response in the frog as studied by intracellular recording. *Vision Res.* **10,** 1093–1100.

Zeise M. L. and Hamdorf K. (1983) Two late response components in on-off ganglion cells of the frog retina. *Vision. Res.* **23,** 887–893.